DETERMINING RADIAL PROFILES FOR PRESTELLAR CORES DETECTED WITH HERSCHEL

by

Ethan James Dederick

A thesis submitted in partial fulfillment of the requirements

for graduation with Honors in Astronomy-Physics.

Whitman College

2014

Certificate of Approval

This is to certify that the accompanying thesis by Ethan Dederick has been accepted in partial fulfillment of the requirements for graduation with Honors in Astronomy-Physics.

_____

Cassandra Fallscheer, Ph.D.

Whitman College

May 12, 2014

Contents

Abstract

Here I investigate the Sersic profiles of prestellar cores in the Cepheus flare star-forming region as detected by the Herschel Space Observatory. Specifically, I desire to know the average value of the Sersic Index that describes the shape of these cores and how it differs from that of a Gaussian profile, if at all. I also investigate whether these cores are more centrally or peripherally concentrated than a Gaussian. Though images were obtained at five different wavelengths, I only perform the analysis on the three images taken at 250 μm, 350 μm, and 500 μm wavelengths. Of the 1121 surveyed cores, I find that they are more centrally concentrated with a mean Sersic Index of 0.694, differing from that of a Gaussian by 0.194.

Ethan James Dederick

Whitman College

May 12, 2014

List of Tables & Figures

I. Introduction

Stars are born from Giant Molecular Clouds (GMC) of dust and gas. Once an equilibrated cloud has been perturbed by some external disturbance, it begins to collapse upon itself. These clouds are often so large that they collapse into several hundred stars or more and become known as star-forming regions. Each collapsing pocket of gas within the GMC will eventually become a star, should it contain enough mass to ignite fusion.

Although the origin of stars is known (molecular clouds), as well as the end result (a fully formed star), far too much information remains in the dark as to how these two stages are bridged. Each step throughout star formation is of great interest and importance, but one in particular fails to be well understood and is the focus of this thesis. This stage, known as a prestellar core, directly follows the initial collapse of the molecular cloud. A prestellar core is, as Anathpindika & Di Francesco (2013) explain, "a gravitationally bound starless core with internal temperatures typically of order a few Kelvin, and a flat central density relative to the protostellar core". A protostellar core, or protostar, is the next stage in star formation following the prestellar core, characterized by gravitational collapse. Finally, temperatures in the core become high enough for fusion to begin and a star is born. It is worth noting here that Anathpindika & Di Francesco (2013) have shown that it is possible for a prestellar core to not evolve into a protostar, but that is beyond the scope of this thesis.

One way in which it is possible to classify pre- and protostellar cores is by examining their radial intensity profiles. Scanning an astronomical region of interest, a telescope with a CCD camera (in this particular case the Herschel Space Observatory) measures intensities of astronomical objects. The light from each object is recorded on a finite number of pixels within the CCD; the brighter the object, the more pixels its light will occupy (assuming fixed distance from the CCD for each object, a safe assumption for the 2.7 kpc distant Cepheus flare). In this way, it is possible to compare relative intensity values between each given pixel in which a particular object of interest is detected.

The images of the Cepheus flare taken by Herschel are of regions 1157, 1172, 1228, 1241, and 1251 from the Lynds catalogue. The Lynds catalogue is a catalogue of dark nebulae created by Beverly Lynds at NRAO in 1962. It contains the equatorial and galactic coordinates of the center of 1802 nebular clouds, the size of the cloud regions (square degrees), and their estimated opacities (Lynds, 1962). These images will further be referred to as L1157, L1172, etc. where L denotes Lynds.

We expect the intensity profile of a prestellar core to be radially dependent. However, the objects themselves are spheroidal though we see them as elliptical in their 2D projections. The radial dependence of these objects therefore follows concentric ellipses of increasing major and minor axes while maintaining a constant ratio between the two (see Figure 1). By then comparing the intensity values of each pixel along the expanding ellipses, a plot of intensity as a function

of radius can be generated, thereby shedding light on the shape of the prestellar core.

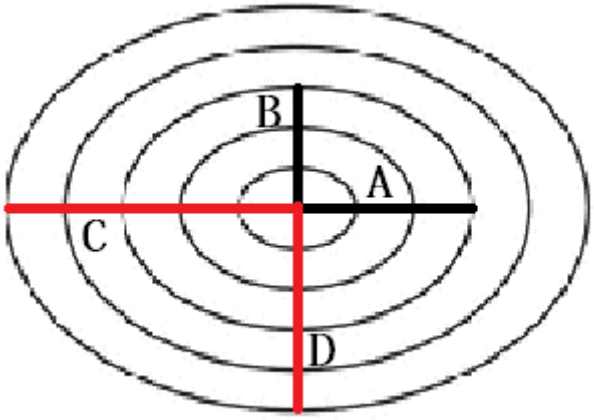

Figure 1:

Concentric ellipses of increasing major and minor axes. Lines A and B represent the semimajor and semiminor axes of one ellipse, respectively. Lines C and D represent the semimajor and semiminor axes of a larger concentric ellipse, respectively. Note how AD=BC.

II. Profile Shape

The general intensity profile of an astronomical object is given by

$$I(r) = I_0 e^{-Rr^{\frac{1}{n}}} \quad (1)$$

where I_0 is the maximum intensity amplitude, R is the inverse radius, r is the elliptical radius, and n is the Sersic Index. For an isothermal sphere, n=0.5, resulting in

$$I(r) = I_0 e^{-Rr^2} \quad (2)$$

which is merely a Gaussian intensity profile (van der Marel, 1999). If the Sersic Index, n>0.5, then the shape of the prestellar core is more centrally concentrated, resulting in an intensity profile that drops off quicker. If n<0.5, then the intensity profile falls off further from the center, resulting in a less concentrated core. See Figure 2 for a visual representation.

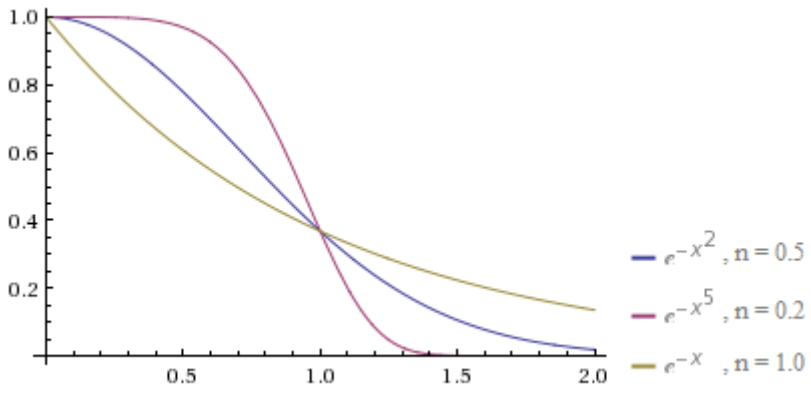

Figure 2:

Three different intensity profiles for varying Sersic Indices. The x^2 exponential corresponds to an index of 0.5, the x^5 exponential corresponds to an index of 0.2, and the x exponential corresponds to an index of 1. Note how the later drop-offs in intensity correspond to lower Sersic Indices and less concentrated cores.

The inverse radius parameter is another way to represent the width of the Gaussian profile. Physicists may be more akin to seeing a Gaussian function in the following form,

$$I(r) = I_0 e^{-(x^2/2\sigma^2)} \tag{3}$$

where σ is the width of the Gaussian. Comparing equations (2) and (3), it becomes clear that

$$R = \frac{1}{2\sigma^2} \quad (4)$$

Thus the inverse radius is an alternate way to describe the width of the intensity profile. The larger σ becomes, the wider the profile. Alternately, the larger the value of the inverse radius, the narrower the intensity profile and the more centrally concentrated the light from the prestellar core.

III. Motivation

The goal of this research is to learn what average Sersic Index value fits prestellar core intensity profiles. I investigate this by analyzing the prestellar populations within five regions of the Cepheus flare. I aim to determine the value of the Sersic Index that describes radial intensity profiles of prestellar cores and whether it differs from Gaussian. I also investigate whether cores tend to be more or less centrally concentrated as well as the spread of the core intensity shape. In doing so I hope to help provide a framework for theorists to follow when modeling prestellar cores in the star formation process.

IV. Observations

The Herschel Space Observatory was launched in May of 2009 as part of the European Space Agency's Horizon 2000 program. It is in a solar orbit at the Earth-Sun L2 Lagrange point at a distance of 1.5 million kilometers from Earth. One of Herschel's objectives is to study stars and dust/gas clouds to better

understand the star formation process. This is made possible with the PACS, SPIRE, and HIFI instruments aboard Herschel and their ability to observe in the far-infrared and submillimeter wavelengths (60-670 microns) (Pilbratt et al., 2010).

The observations were made by the Herschel Space Observatory of the Cepheus Flare – a giant molecular cloud in the constellation Cepheus – (see Figure 3) as part of the Herschel Gould Belt Survey (André et al., 2010). The observations were conducted sporadically throughout late 2009 to mid-2011. Five regions were scanned within the Cepheus Flare: L1157, L1172, L1228, L1241, and L1251. Each region was observed at five different wavelengths by either the PACS or the SPIRE instrument aboard Herschel. PACS (Photodetector Array Camera and Spectrometer) (Poglitsch et al., 2010) imaged at 70 μm and 160 μm wavelengths while SPIRE (Spectral and Photometric Imaging Receiver) (Griffin et al., 2010) scanned at 250, 350, and 500 μm. PACS and SPIRE scanned at either 20 or 60 arcseconds per second. That equates to roughly a one hour observation for a 1° x 1° field. Details about these observations are given in Table 1.

Table 1:

Locations, instrument observations, scan speeds, and observation dates of Cepheus Flare Herschel Images (Fallscheer et al., 2014).

Field	Right Ascension (degrees)	Declination (degrees)	Observation Type (Spire/Pacs)	Scan Speed (arcsec/s)	Observation Date
L1157	310.266	67.580	SpP	60	1 Feb 2010
L1157	310.267	67.580	P	20	27 Jul 2011
L1172	315.461	67.775	SpP	60	19 Feb 2010
L1172	315.461	67.775	P	20	3 Jun 2010
L1228	314.566	77.547	SpP	60	22 Jun 2010
L1228	314.567	77.546	P	20	22 Jun 2011
L1241	329.600	76.734	SpP	60	28 Dec 2009
L1241	329.600	76.734	P	20	3 Jun 2010
L1251	337.500	75.176	SpP	60	28 Dec 2009
L1251	337.500	75.176	SpP	60	25 Jan 2010
L1251	337.499	75.176	P	20	29 Jun 2011

Figure 3:

The Cepheus Flare star-forming region in the constellation Cepheus. (Image courtesy of Adam Block taken at the Mt. Lemmon SkyCenter.)

Following acquisition, the data were reduced using HIPE (Herschel Interactive Processing Environment) (Ott, 2010) version 7.0.0. More specifically, the SPIRE data were reduced and calibrated with the SPIA package and SPIRE_CAL 6.1, respectively (Schulz, 2011). The PACS data were reduced using a Python script and calibrations were obtained with the Planck Telescope at each PACS wavelength. The image maps at each wavelength were created using Scanamorphos (Roussel, 2013) and absolute flux calibration was obtained through comparison of these images with Planck and IRAS data (Abergel et al., 2014).

Finally, a source catalog was produced for each image using getSources version 130401. GetSources is a multi-wavelength, multi-scale source extraction algorithm (Men'shchikov et al., 2012). Each wavelength of the Scanamorphos maps was run through the algorithm (see Figure 4), producing a final catalog for each region with the corresponding number of sources listed in Table 2.

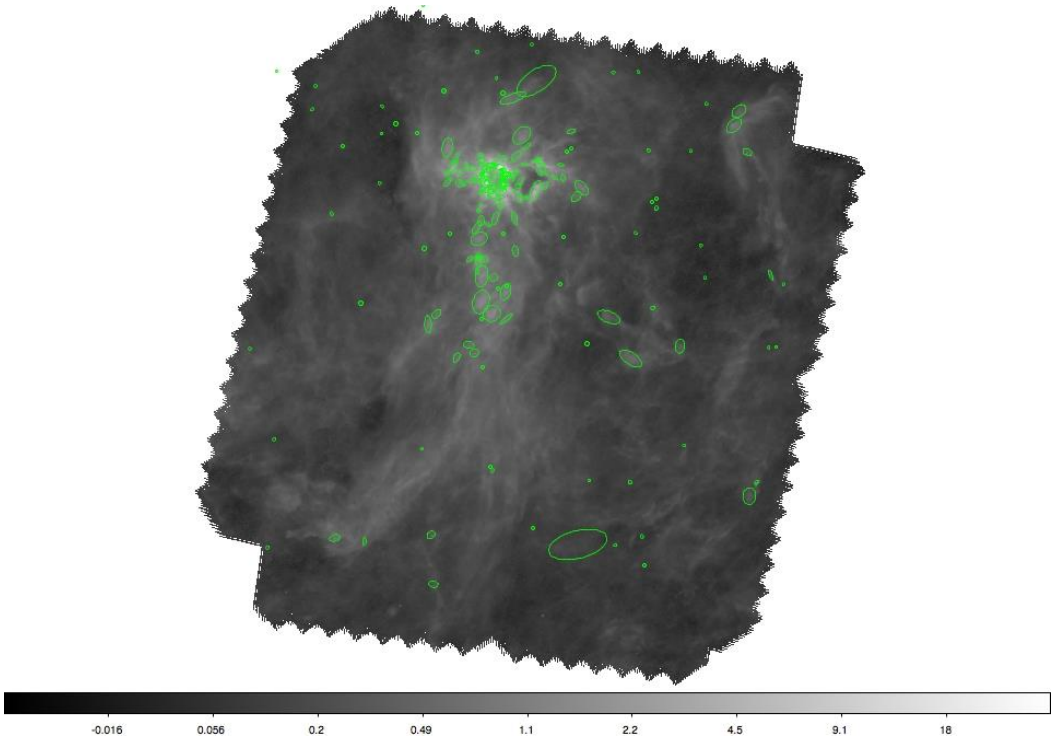

Figure 4:

Image L1172 after running the getSources software. The ellipses are identified prestellar cores (Fallscheer et al., 2014).

Table 2:

Number of sources per image.

Image	Number of Sources
L1157	172
L1172	299
L1228	283
L1241	129
L1251	238

V. Analysis

The procedure for determining the Sersic Indices of the prestellar cores is as follows:

1) Using the getSources catalogue, identify the location and size of each core's elliptical footprint.
2) Plot the intensity values of each pixel as a function of its elliptical radius from the core center.
3) Fit a Sersic profile to the data and record the Sersic Index.
4) Compile the index from each core into histograms for each wavelength, each image, and then a combination of all images and wavelengths.

The code necessary to perform these tasks is written in IDL script using Whitman College's IDL license. For further information about the code itself, please see Appendix I where the code is listed verbatim.

Before any discussion of analysis begins, it should be noted that the images taken by the PACS instrument (λ=70, 160 μm) are not included in the analysis. The PACS images are of lower sensitivity and therefore the corresponding intensity plots are unsuitable for accurate analysis. Therefore, only images taken in the 250, 350, and 500 μm wavelengths are included in the following discussion.

Another disclaimer regarding the number of sources in each image should be noted. In addition to the prestellar cores, getSources also identified any objects that fit the algorithmic description of a core. Some of these objects could actually be distant background galaxies or error. Therefore, I manually viewed each intensity plot to decide which objects were actually cores and which were not. Those that are not included in the analysis demonstrated either a complete lack of discernable structure (Figure 5) or a roughly uniform intensity across all radii (Figure 6). Thus it should be noted that the number of objects included in the final analysis is actually less than the values given in Table 2.

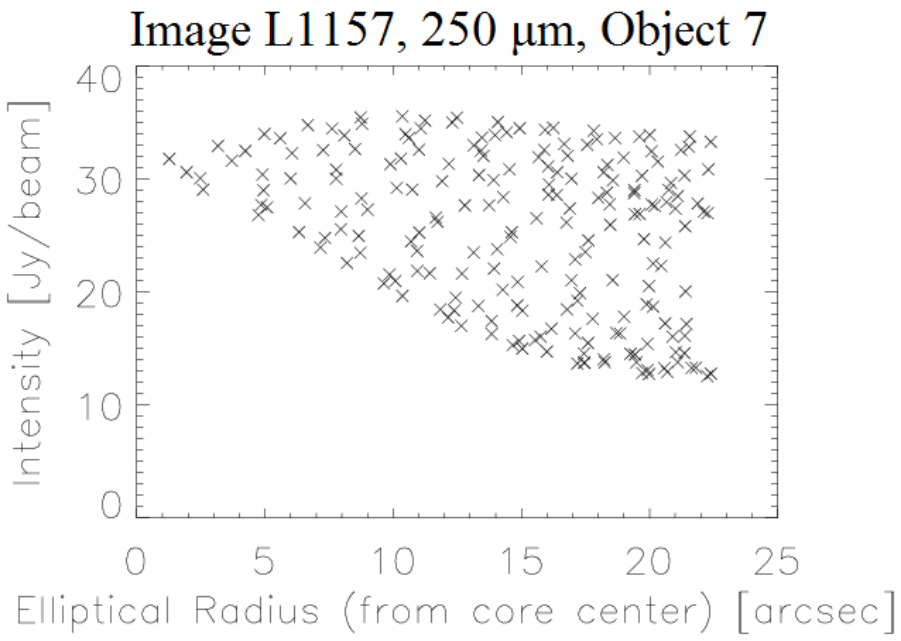

Figure 5:

An example of an object not included in analysis. There is no discernable intensity profile and is therefore an object misidentified as a prestellar core.

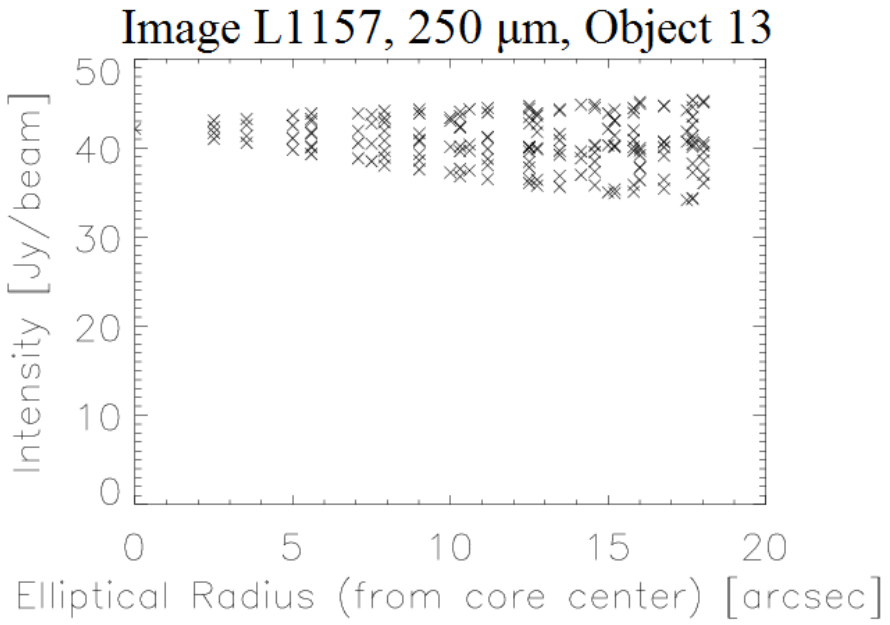

Figure 6:

An example of an object not included in analysis. The object displays a roughly uniform intensity across all radii, characteristic of background noise rather than a prestellar core.

A typical intensity distribution of a prestellar core is provided in Figure 7. The vertical axis is given in units of Janskys per beam where 1 Jansky = 10^{-23} erg s^{-1} cm^{-2} Hz^{-1}. Although these happen to be the units, the concern of the plot is the shape of the distribution rather than the absolute intensity. In truth, this axis could have arbitrary intensity units for the shape of the profile would remain unchanged. The structure of the distributions vary wildly from core to core, but all can be well-fitted with the intensity profile given in equation (1).

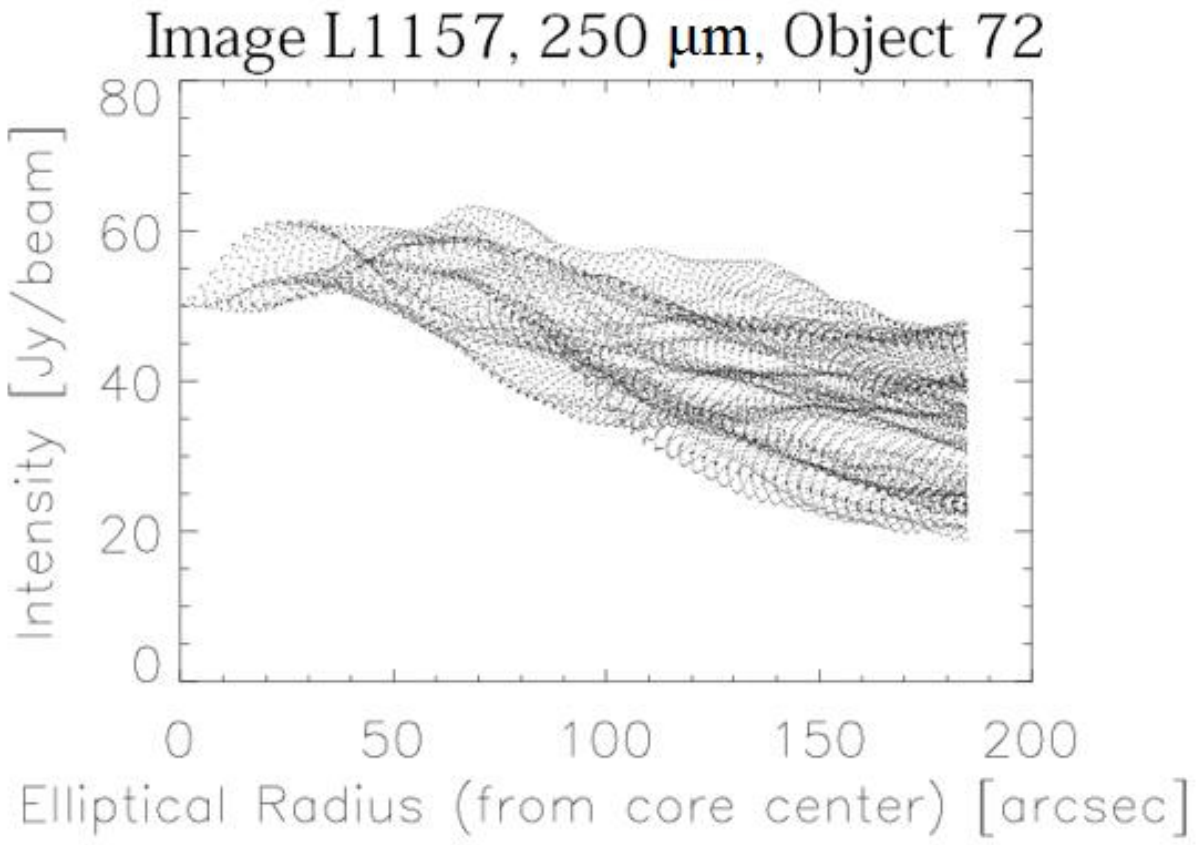

Figure 7:

A typical intensity distribution for a prestellar core. The displayed core is object 72 from image L1157 taken in 250 nm. The horizontal axis is the radial distance from core center in arcseconds and the vertical axis is the intensity in Janskys per beam.

The algorithm to find the fitted Sersic profile begins with initial guesses for the amplitude, inverse radius, and Sersic Index. The initial guess for the maximum amplitude is the maximum intensity value of the distribution; the initial guess for the inverse radius is 2 divided by the major axis full width half maximum; and the initial guess for the Sersic Index is 1. IDL then recursively modifies its guesses until it finds an appropriate profile.

I then record each Sersic Index from each distribution and compile them into readable text files. Those files are then accessed by IDL's histogram function (see Appendix 1, subsection II) to create histograms of the frequency of Sersic Indices for each individual wavelength in each of the five regions, then a combination of all wavelengths for each region, and finally a combined histogram of all data on hand. For a visual representation of these histograms, please refer to Figure 8. The Sersic Indices are plotted in bins of 0.05. To analyze the distribution of Sersic Indices of the cores, I fit a Gaussian distribution to the histograms where the peak corresponds to the index of greatest frequency. The Gaussian is only fit to the data between an index of 0.2 and an index of 1.5. Fitting to values greater than 1.5 would result in a skewed profile. Fitting to all values would require a non-Gaussian function indicating an average that is skewed from the clearly dominant Sersic Indices.

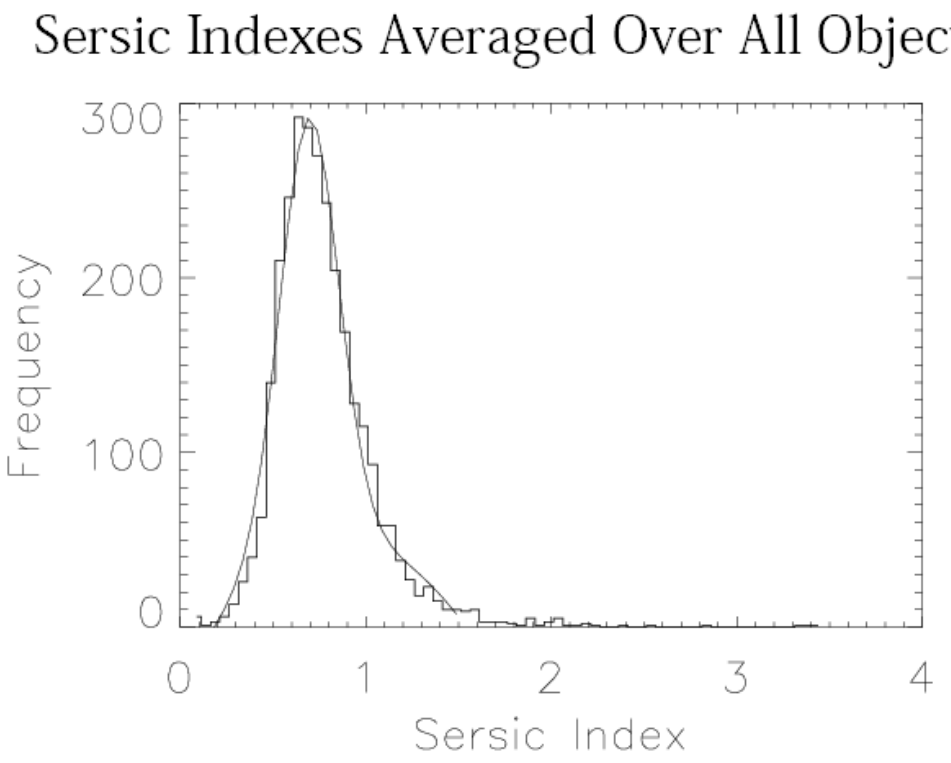

Figure 8:

The compilation of all Sersic Indices from all objects in all images at all wavelengths. The bin sizes of the Sersic Indices are 0.05. The stepped solid line represents the data and the smooth solid line is the Gaussian fit for the histogram between indices of 0.2 and 1.5.

The results of the most frequently observed Sersic Indices are listed in Table 3. I find that for selected regions, the average Sersic Indices of the prestellar cores fall within 0.429 to 0.998. However, the overall average Sersic Index is 0.694, and therefore not Gaussian. There are instances of significantly larger Sersic Indices around 2 or 3, but those are rare cases.

As the average Sersic Index of the prestellar cores is larger than 0.5, these cores are more centrally concentrated than the Gaussian. This will help give theorists a modeling guideline for prestellar core structure in stellar evolution.

Additionally, the spread of the distribution of Sersic Indices runs from 0.2 to 1.5 for those within the histogram's Gaussian fit. The fit has a full width half maximum of 0.4, approximately 30% of the full spread, indicating a narrow Gaussian with the vast majority of Serisc Indices falling between 0.5 and 0.9.

Table 3:

Average Sersic Index for each wavelength in each image and the compiled totals.

Image	Wavelength (μm)	Avg. Sersic Index
L1157	250	0.778
	350	0.429
	500	0.633
	Combined	0.661

Image	Wavelength (μm)	Avg. Sersic Index
L1172	250	0.717
	350	0.634
	500	0.593
	Combined	0.642

Image	Wavelength (μm)	Avg. Sersic Index
L1228	250	0.770
	350	0.761
	500	0.685
	Combined	0.740

Image	Wavelength (μm)	Avg. Sersic Index
L1241	250	0.998
	350	0.717
	500	0.645
	Combined	0.712

Image	Wavelength (μm)	Avg. Sersic Index
L1251	250	0.910
	350	0.679
	500	0.657
	Combined	0.716

Image	Wavelength (μm)	Avg. Sersic Index
All	All	0.694

VI. Conclusion

Here I have demonstrated using data taken from Herschel that, at least in the Cepheus flare star-forming regions, the majority of prestellar cores do not assume a Gaussian profile. Instead, they assume an intensity distribution with a Sersic Index closer to 0.69. Cases of abnormally high (n=2-3) Sersic Indices are also observed, but the vast majority of sources are best fit by a Sersic Index between 0.4 and 0.9. As such, the prestellar cores exhibit a more centrally concentrated distribution/shape. Further research on other star-forming regions is encouraged to reaffirm or refute these findings.

VII. Appendix I

The code used for this project is written in IDL, or Interface Definition Language. IDL defines capabilities of a distributed service along with common data type sets to interact with the distributed services. It is an independent interface language meaning it can function without exterior programs. IDL is a language created in 1977 that has a wide range of applications, but is very common in applications of astronomy.

Here I present code used to perform the analysis discussed in Section V. The code is laid out in the following subsections based on purpose.

I. Read in the Catalogue, Plot an Intensity Distribution, Fit a Sersic Profile

```
pro LOOPWITHGRAPHS
;This program reads in the GetSources catalogs and creates an intensity plot for
all the prestellar cores in the catalogue.

; Load catalogs
directory='/home/dederiej/Herschel/getsources2013apr/'
source ='cep1157'
catname='cep1157'

;Pathway to the directory
gspath=directory+source
gs='.sw.final.reliable.ok.cat'
gscat=gspath+gs

;Read catalogue values
;xcenter is 1st D, ycenter is 2nd D
fmt=
'I,D,D,X,X,X,X,X,X,X,X,X,X,X,X,X,X,X,X,X,X,X,X,X,X,X,X,X,X,X,X,X,X,X,X,X,X,X,D,
D,D,X,X,X,X,X,X,X,X,X,X,X,X,X,X,X,X,X,X,X,X,X,X,X,X,X,X,X,X,X,X,X,X,X,X,X,X,X'

;These are the values read in from above, skipping readcol and gscat
```

```
readcol, gscat, catnum,xcop,ycop,a4fwhm,b4fwhm,theta4, comment='#',
format=fmt, skipline=151


;Maximum pixel values of image
picturex=3001
picturey=2984

;Number of arcsec per pixel
arcy=2.5


;Minimum pixel values of image
pixelx=1
pixely=1


;Read in image
image=readfits("~/Herschel/bigimages/cep1157_spire_250_scanam.image.resa
mp.r19p5.fits")

;Loop over all objects in image
for k=1,n_elements(catnum)-1 do begin

;Center of object
xcenter=xcop[k]
ycenter=ycop[k]

;Semimajor and semiminor axes of object in arcsec
major=a4fwhm[k]
minor=b4fwhm[k]

;Convert semimajor and semiminor axes from arcsec to pixels
majorFWHMpixel=major/arcy
minorFWHMpixel=minor/arcy

;Angle of object relative to vertical (East of North)
t=theta4[k]
angle=t*(2.0*!Pi)/360.0


;Define empty arrays to fill with image values for ellipse
ellipse=[ ]
pixvals=[ ]
```

```
maxis=[ ]


;Loop through all pixels in the image to find which ones are within ellipse and get
;intensity values for those pixels
for I=pixelx,picturex do begin
      for J=pixely,picturey do begin
            if ((xcenter-I)*sin(angle)+(J-
ycenter)*cos(angle))^2/majorFWHMpixel^2+((I-xcenter)*cos(angle)+(J-
ycenter)*sin(angle))^2/minorFWHMpixel^2 le 1.0 then begin
            ellipse=[[ellipse],[I,J]]
            pixvals=[[pixvals],[image[I,J]]]
            a=sqrt(((xcenter-I)*sin(angle)+(J-
ycenter)*cos(angle))^2+(major/minor)^2*((I-xcenter)*cos(angle)+(J-
ycenter)*sin(angle))^2)
            maxis=[[maxis],[a]]
            endif
      endfor
endfor

;Change pixel values back to arcsec from center of object
maxis=maxis*arcy


;Plot object image values as function of distance (arcsec) from center
plot,maxis,pixvals,title='Radial Profile (Image 1, Object 16, 250
nm)',xtitle='Elliptical Radius (from core center) [arcsec]',ytitle='Intensity
[Jy/beam]',charsize=2,psym=3

;Fitting coding (initial guesses for recursive fitting)
parinfo = replicate({limited:[0,0],limits:[0,0]},3)
parinfo(0).limited(0) = 1
parinfo(0).limited(1) = 1
parinfo(0).limits(0) = 1.0d
parinfo(0).limits(1) = 4.0d
parinfo(1).limited(0) = 1
parinfo(1).limited(1) = 1
parinfo(1).limits(0) = 5.0d
parinfo(1).limits(1) = 80.0d


coefs=fltarr(3,2)
initguess=[max(pixvals),2.0/majorFWHMpixel,1.0]
errArr=sqrt(pixvals)
```

```
;Fit an intensity profile to the plot by calling Sersic function
fit=mpfitfun('sersic',maxis,pixvals,errArr,initguess)
coefs(0,0)=fit(0)
coefs(1,0)=fit(1)
coefs(2,0)=fit(2)

print,coefs(0,0)
print,coefs(1,0)
print,coefs(2,0)

p=[coefs(0,0),coefs(1,0),coefs(2,0)]

sersic=sersic(maxis,p)

;Overlay fitted intensity profile on plot
oplot,maxis,sersic
endfor
end
```

The sersic fitting function is referenced in the code above. Its code is as follows:

```
function sersic, rin, p

;p are the three parameters to be fit

amp     = p[0]       ;guess for the amplitude
invr    = p[1]       ;guess for the inverse radius
ser     = p[2]       ;guess for the sersic index

;Return the final fit
return, rad_val
end
```

II. Plot a Histogram for a Particular Image

```
pro Histogram

;Set bin size
sizing=.05

;Read in text file with data
readcol,'Image1251_500good.txt',sersicindex,flag,format='f,a'

;Read only the good data values
gooddata=sersicindex[where(flag eq '*')]

;Define a histogram
result=histogram(gooddata,binsize=sizing)
bins=(findgen(n_elements(result)))*sizing+min(gooddata)

;Plot the histogram and fit a Gaussian profile
plot,bins,result,charsize=2,/nodata,xtitle='Sersic Index',ytitle='Frequency'
oplot,bins,result,psym=10,linestyle=0,thick=2
yfit=gaussfit(bins(where(bins lt 1.3)),result(where(bins lt 1.3)))
oplot,bins,yfit

;Plot the histogram with fit to .PS file
!P.MULTI=[0,1,1]
set_plot, 'PS'
device, filename='Histogram1251_500.ps',/encapsulated
plot,bins,result,charsize=2,/nodata,xtitle='Sersic Index',ytitle='Frequency'
oplot,bins,result,psym=10,linestyle=0,thick=2
yfit=gaussfit(bins(where(bins lt 1.3)),result(where(bins lt 1.3)),A)
oplot,bins,yfit
device,/close_file
set_plot, 'x'

end
```

References

Abergel, A. et al., 2014, arXiv: 1312.1300v2, p.1.

Anathpindika, S., & Di Francesco, J., 2013, MNRAS 430.185, 4A.

André, P. et al., 2010, A&A 518L, 102A.

Fallscheer, C. et al., 2014, *in preparation*.

Griffin, M. et al., 2010, A&A 518L, 3G.

Lynds, B., 1962, ApJ 7, 1L.

Men'shchikov, A. et al., 2012, A&A 542A, 81M.

Ott, S., 2010, ASPC 434, 139O.

Pilbratt, G. et al., 2010, A&A 518, L1.

Poglitsch, A. et al., 2010, A&A 518L, 2P.

Roussel, H., 2013, PASP 125, 1126R.

Schulz, B., 2011, ASPC 442, 691S.

Van der Marel, R., 1999, ASPC 182, 65V.